Coherent population oscillation produced by saturating probe and pump fields on the intercombination line

A. Vafafard,[1,2,*] M. Mahmoudi,[2] and G. S. Agarwal[1]
[1]*Department of Physics, Oklahoma State University, Stillwater, Oklahoma 74078, USA*
[2]*Department of Physics, University of Zanjan, University Blvd., 45371-38791 Zanjan, Iran*
(Received 26 January 2016; published 28 March 2016)

We present a theoretical study of the experiments on coherent population oscillations and coherent population trapping on the intercombination line of ^{174}Yb. The transition involves a change of the spin and thus can not be interpreted in terms of an effective lambda system. The reported experiments are done in the regime where both pump and probe fields can saturate the transition. We demonstrate, by both numerical and analytical calculations, the appearance of the interference minimum as both pump and probe start saturating the transition. We present an analytical result for the threshold probe power required for the interference minimum to appear. We also present a detailed study of the appearance of the interference minimum when magnetic fields are applied. The magnetic fields not only create Zeeman splittings, but in addition make the system open because of the couplings to other levels. We show the possibility of interference minimums at the position of subharmonic resonances.

DOI: 10.1103/PhysRevA.93.033848

I. INTRODUCTION

Atomic coherence effects, induced by laser fields, such as the coherent population trapping (CPT) [1], the coherent population oscillation (CPO) [2], and the electromagnetically induced transparency (EIT) [3] have become increasingly popular because of their wide range of applications in areas, such as lasing without inversion [4], enhancement of the refractive index [5], slow light [6–8], storage of light [9,10], nanoscale resolution [11], magnetometry [12], etc. These applications typically use a narrow dip in the absorption spectra produced by interference due to multiple pathways. The atomic coherence effects in single electron atoms like Na, ^{85}Rb, and Cs have been extensively studied. Results for both coherent population trapping and coherent population oscillations are available [13–17]. Compared to single-electron atoms, there have been few studies for two-electron atoms. In the investigation of a two electron system, one needs to take into account the Pauli exclusion principle to obtain the allowed transitions. Maynard *et al.* [10] studied the transition $2\,^3S_1 \rightarrow 2\,^3P_1$ in metastable He, which is a Λ system. They observed CPO between two levels involving only a change of spin. Mompart *et al.* have presented a study of CPT in a two-electron atom with aligned spins [18]. They specifically studied the transitions in a two electron wave function where both ground and excited states had aligned spins (ortho system); thus the orbital part of the two electron system was antisymmetric. It revealed the possibility that an ortho system can show CPT, such as in the transition of $4s4p$ to $4p4p$ in Ca, a V system. This is due to the Pauli Principle in that the V system becomes equivalent to a Λ system [19]. In a recent experimental work, Singh and Natarajan studied the intercombination line $^1S_0 \rightarrow {}^3P_1$ in ^{174}Yb [20]. They reported both CPO and CPT in such a system. They also reported these coherent effects in presence of a magnetic field.

The purpose of this paper is to understand the experimental results and to delineate the physical mechanisms leading to the occurrence of both CPO and CPT in the intercombination transition. Such a transition forms a V system and hence the observation of CPO or CPT is surprising. It is to be noted that for the observation of CPO in two level atoms, there is a need for strong dephasing [14]. An atomic beam has no dephasing; hence the observation of CPO in an atomic beam experiment is quite remarkable. The authors of Ref. [20] indicated that their experimental observation could be understood in terms of the theoretical model of Mompart *et al.* [18]. However the ground and excited states for the intercombination line have a different spin configuration than in the work of Mompart *et al.* which studies a transition with no change in spin. For the transition $^1S_0$-$^3P_1$ in ^{174}Yb, the ground state has two spins which are antiparallel whereas the excited state has two spins which are parallel. Therefore, there is a need for a theoretical model that can explain the experimental results on the intercombination line. This paper will develop a theoretical model to explain the experimental observations.

It is worth noting that unlike most pump and probe experiments, the study of Ref. [20] used a pump and a probe with comparable intensities. This is unique to this experiment and gives evidence that the probe is not weak compared to the pump; thus the saturation of the transition by both pump and probe fields is expected to have major effects. This must be accounted for any theoretical modeling. Our major finding is that the saturation of the transition by both pump and probe fields explains the experimental data.

The paper will be organized in the following way. In Sec. II we describe the intercombination line as an effective four level system with the ground and excited states coupled by pump and probe fields which are orthogonally polarized and have comparable intensities. We derive the basic density matrix equations and present the expressions for the fluorescence. In Sec. III we present numerical results for fluorescence obtained from a Floquet analysis. The results are shown in the absence of the magnetic field and in presence of the magnetic field. Our numerical results confirm the behavior as observed in experiments. In Sec. IV we present a number of analytical results when the magnetic field is zero. The analytical results help us to understand the observed behavior of fluorescence. In Sec. V we present our conclusions.

*azar.vafafard@okstate.edu

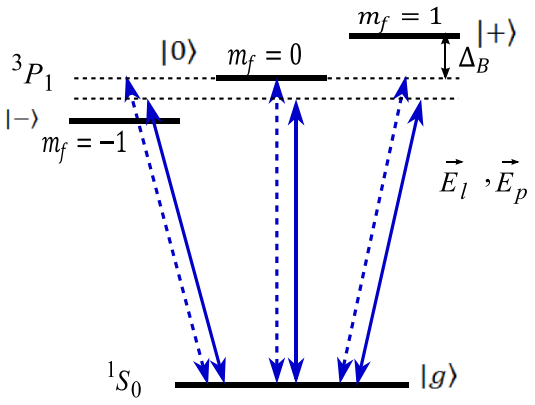

FIG. 1. Two-electron, four-level quantum system driven by two orthogonally polarized laser fields, the probe $\vec{E}_p$ (solid) and pump $\vec{E}_l$ (dashed) fields. As indicated in the text, these couplings with the lasers are effective couplings.

II. MODEL AND EQUATIONS

A two-electron atomic model is considered as shown in Fig. 1. The ground state is $|g\rangle = {}^1S_0\,(F=0, M_f=0)$ and the upper levels are shown as $|-\rangle = {}^3P_1\,(F=1, M_f=-1)$, $|0\rangle = {}^3P_1\ (F=1, M_f=0)$, and $|+\rangle = {}^3P_1\,(F=1, M_f=1)$. The transition used is the ${}^1S_0 \rightarrow {}^3P_1$ at the 556 nm intercombination line of the even isotope ^{174}Yb atom. The state ${}^3P_1$ is weakly mixed to transition ${}^1P_1$ which has two spins antiparallel. Thus *effectively*, we can think that the level ${}^3P_1$ is coupled to the level ${}^1S_0$ via the laser field. Two orthogonal linearly polarized fields, $\vec{E}_p$ as the probe field and $\vec{E}_l$ as the pump field, couple the ground level to the upper levels :

$$\begin{aligned}\vec{E}_p &= \varepsilon_p(\sin\theta\hat{x} + \cos\theta\hat{z})e^{-i\omega_p t + ik_p y} + \text{c.c.},\\ \vec{E}_l &= \varepsilon_l(\cos\theta\hat{x} - \sin\theta\hat{z})e^{-i\omega_l t + ik_l y} + \text{c.c.},\\ \vec{E}_p &\cdot \vec{E}_l = 0,\end{aligned} \tag{1}$$

where ε_p and ε_l are the probe and pump field amplitudes, respectively; and θ shows the angle between the polarization of the probe and direction of the propagation of the atomic beam. The Rabi frequencies of the probe and pump fields can be defined as $2\Omega_{pi} = 2[\varepsilon_p(\sin\theta\hat{x} + \cos\theta\hat{z})]\cdot \vec{d}_{ig}/\hbar$, and $2\Omega_{li} = 2[\varepsilon_l(\cos\theta\hat{x} - \sin\theta\hat{z})]\cdot \vec{d}_{ig}/\hbar (i = +,0,-)$. The dipole matrix element $\vec{d}_{ig}$ can be written using Clebsch-Gordan coefficients as

$$\vec{d}_{+g} = |d|\hat{\epsilon}_+, \quad \vec{d}_{0g} = |d|\hat{z}, \quad \vec{d}_{-g} = |d|\hat{\epsilon}_-, \tag{2}$$

where $|d|$ is the reduced dipole matrix element and $\hat{\epsilon}_\pm = (\hat{x} \pm i\hat{y}/\sqrt{2})$. It should be borne in mind that the parameter d would include the coefficient of mixing with the level ${}^1P_1$. Using Eq. (2), the Rabi frequencies can be expressed as

$$\begin{aligned}\Omega_{p+} = \Omega_{p-} &= \frac{A_p}{\sqrt{2}}\sin\theta, \quad \Omega_{p0} = A_p\cos\theta,\\ \Omega_{l+} = \Omega_{l-} &= \frac{A_l}{\sqrt{2}}\cos\theta, \quad \Omega_{l0} = -A_l\sin\theta,\end{aligned} \tag{3}$$

where $A_p = |d|\varepsilon_p$ and $A_l = |d|\varepsilon_l$. We use the same geometry as in [20], i.e., the atomic beam is moving in direction z and the lasers are propagating perpendicularly to the direction of the atomic beam. The Hamiltonian of the system interacting with two laser fields in the dipole and rotating wave approximations is given by

$$H_{in} = -\hbar\left\{\left[\sum_{j=+,0,-}(\Omega_{pi}e^{-i\omega_p t} + \Omega_{li}e^{-i\omega_l t})|j\rangle\langle g|\right] + \text{c.c.}\right\}, \tag{4}$$

where ω_p and ω_l denote the frequencies of the applied fields. In the rotating frame, the density matrix equations, which show the response of the medium to the field, are given by

$$\begin{aligned}\dot{\rho}_{++} &= i\rho_{g+}(\Omega_{p+}e^{-i\Delta t} + \Omega_{l+}) - i\rho_{+g}(\Omega_{p+}e^{i\Delta t} + \Omega_{l+})\\ &\quad - \gamma_{+g}\rho_{++},\\ \dot{\rho}_{00} &= i\rho_{g0}(\Omega_{p0}e^{-i\Delta t} + \Omega_{l0}) - i\rho_{0g}(\Omega_{p0}e^{i\Delta t} + \Omega_{l0})\\ &\quad - \gamma_{0g}\rho_{00},\\ \dot{\rho}_{--} &= i\rho_{g-}(\Omega_{p-}e^{-i\Delta t} + \Omega_{l-}) - i\rho_{-g}(\Omega_{p-}e^{i\Delta t} + \Omega_{l-})\\ &\quad - \gamma_{-g}\rho_{--},\\ \dot{\rho}_{g+} &= -i\delta_+\rho_{g+} + i(\rho_{++} - \rho_{gg})(\Omega_{p+}e^{i\Delta t} + \Omega_{l+})\\ &\quad + i\rho_{0+}(\Omega_{p0}e^{i\Delta t} + \Omega_{l0}) + i\rho_{-+}(\Omega_{p-}e^{i\Delta t} + \Omega_{l-})\\ &\quad - \Gamma_{g+}\rho_{g+},\\ \dot{\rho}_{g0} &= -i\delta_0\rho_{g0} + i(\rho_{00} - \rho_{gg})(\Omega_{p0}e^{i\Delta t} + \Omega_{l0})\\ &\quad + i\rho_{+0}(\Omega_{p+}e^{i\Delta t} + \Omega_{l+}) + i\rho_{-0}(\Omega_{p-}e^{i\Delta t} + \Omega_{l-})\\ &\quad - \Gamma_{g0}\rho_{g0},\\ \dot{\rho}_{g-} &= -i\delta_-\rho_{g-} + i(\rho_{--} - \rho_{gg})(\Omega_{p-}e^{i\Delta t} + \Omega_{l-})\\ &\quad + i\rho_{+-}(\Omega_{p+}e^{i\Delta t} + \Omega_{l+}) + i\rho_{0-}(\Omega_{p0}e^{i\Delta t} + \Omega_{l0})\\ &\quad - \Gamma_{g-}\rho_{g-},\\ \dot{\rho}_{0+} &= -i(\delta_+ - \delta_0)\rho_{0+} - i\rho_{0g}(\Omega_{p+}e^{i\Delta t} + \Omega_{l+})\\ &\quad + i\rho_{g+}(\Omega_{p0}e^{-i\Delta t} + \Omega_{l0}) - \Gamma_{0+}\rho_{g0},\\ \dot{\rho}_{-+} &= i(\delta_- - \delta_+)\rho_{-+} + i\rho_{g+}(\Omega_{p-}e^{-i\Delta t} + \Omega_{l-})\\ &\quad - i\rho_{-g}(\Omega_{p+}e^{i\Delta t} + \Omega_{l+}) - \Gamma_{-+}\rho_{-+},\\ \dot{\rho}_{-0} &= i(\delta_- - \delta_0)\rho_{-0} + i\rho_{g0}(\Omega_{p-}e^{-i\Delta t} + \Omega_{l-})\\ &\quad - i\rho_{-g}(\Omega_{p0}e^{i\Delta t} + \Omega_{l0}) - \Gamma_{-0}\rho_{-0},\end{aligned} \tag{5}$$

where γ_{ig} is the spontaneous decay rate from level $|i\rangle$ to level $|g\rangle$. The off-diagonal element ρ_{ij} decays at the rate $\Gamma_{ij} = (\gamma_{ig} + \gamma_{jg})/2$. The parameter $\Delta = \omega_p - \omega_l$ denotes the probe field detuning with respect to the pump field. Also $\delta_i = \omega_l - \omega_{ig}(i = +,0,-)$ is the pump field detuning with the atomic resonance transition. Because of the explicit time dependence in Eq. (5), the steady state has the following Floquet expansion:

$$\rho_{ij} = \sum_{m=-\infty}^{\infty}\rho_{ij}^{(m)}e^{-im\Delta t}, \tag{6}$$

where $m = 0$ denotes the time-independent component of the density matrix elements. The positive frequency part of the

electric field operator at the detector is [21]

$$\vec{E}^{(+)}(\vec{r},t) = -\frac{\omega_l^2}{c^2}\vec{n}\times[\vec{n}\times\vec{d}]\frac{e^{ik_l r - i\omega_l t}}{r}e^{-ik_l\vec{n}.\vec{R}}, \quad (7)$$

where the dipole moment operator is given by

$$\vec{d} = \sum_{i=+,0,-}\vec{d}_{gi}\,|g\rangle\langle i|, \quad (8)$$

and $\vec{r}$ denotes the point at which the fluorescence is measured. The atomic sample is located at $\vec{R}$; and $\vec{n} = \frac{\vec{r}}{r}$ is the direction of the observation. According to the experimental setup, the fluorescence is collected in the direction perpendicular to the atomic beam and the laser beams, i.e., in the x direction. The fluorescence is given by

$$I = \langle\vec{E}^{(-)}(\vec{r},t).\vec{E}^{(+)}(\vec{r},t)\rangle, \quad (9)$$

where $\vec{E}^{(-)}$ denotes the negative frequency part of the electric field operator at the detector. With $\vec{n}$ set to the x direction in Eq. (8), the dc component of the fluorescence can be written as

$$I = \frac{I_0}{2}\left[2\rho_{00}^0 + \rho_{++}^0 + \rho_{--}^0 - \rho_{+-}^0 - \rho_{-+}^0\right], \quad (10)$$

where the constant I_0 depends on ω_l and $|d|$. Henceforth, fluorescence will be referred to in units of I_0. It should be noted that the fluorescence has contributions from excited state populations $I_p = \frac{I_0}{2}(2\rho_{00}^0 + \rho_{++}^0 + \rho_{--}^0)$, as well as coherences $I_c = -\frac{I_0}{2}(\rho_{+-}^0 + \rho_{-+}^0)$.

III. NUMERICAL RESULTS

Equations (5) for the density matrix elements are numerically solved using Eq. (6). Note that equations for $\rho_{ij}^{(m)}$ get coupled to $\rho_{ij}^{(m\pm1)}$. Convergence of the truncation is tested for each set of parameters. As in the experiment, the pump is set at resonance ($\delta_0 = 0$), and the probe is scanned (Δ is varied). All parameters are scaled in units of the natural line width $\gamma = 2\pi \times 185$ KHz for the ^{174}Yb intercombination line. Furthermore, $\gamma_{\pm g} = \gamma_{0g} = \gamma$.

We first describe the results in the absence of the magnetic field. In Figs. 2 and 3, we show the fluorescence as a function of the probe detuning $\Delta \geqslant 0$ as $I(-\Delta) = I(+\Delta)$. Typically pump and probe experiments are done for a weak probe and strong pump. We first fix the Rabi frequency of the pump value at which the transition can be saturated ($A_l = 2\gamma$). Fluorescence I (in units of I_0) is shown in Fig. 2 for different strengths of the probe field. Note that for $\theta \neq \pi/4$, the strength of the pump and probe varies according to the transition. For example, the $|g\rangle \rightarrow |0\rangle$ transition has a probe (pump) Rabi frequency proportional to $\cos\theta$ ($\sin\theta$). The polarization angle greatly impacts the fluorescence results as compared in Figs. 2(a), 2(b), and 2(c) with angles $\theta = \pi/6, \pi/4, \pi/3$, respectively. As the strength of the probe increases, a minimum at $\Delta = 0$ starts to appear. For $\theta = \pi/4$, the minimum at $\Delta = 0$ is most pronounced when the pump and probe strengths are comparable. In the experiment [20], the fluorescence was studied for comparable intensities of the pump and probe. Our numerical results for $A_p \sim A_l$ are in agreement

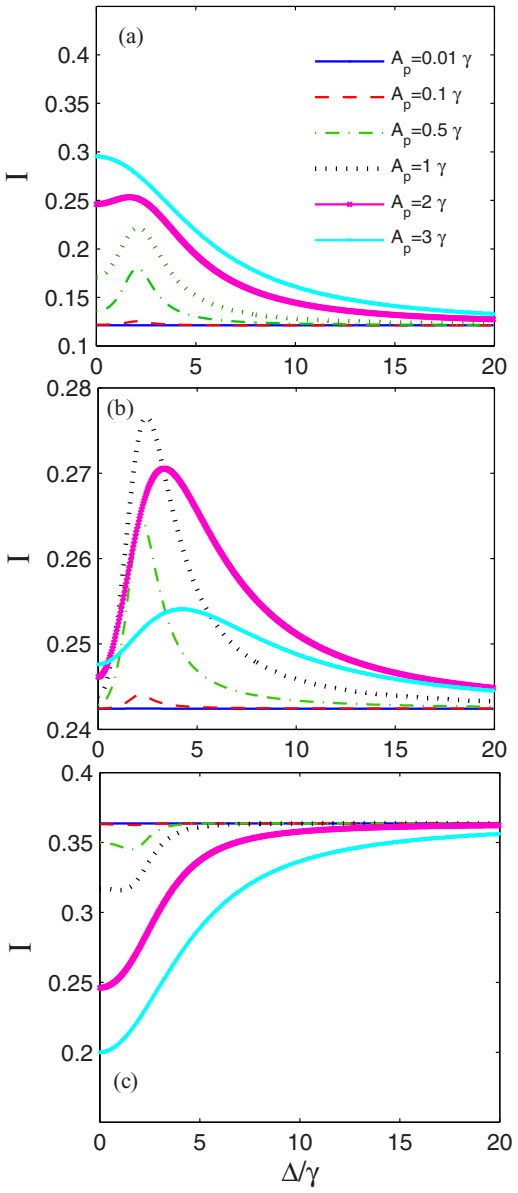

FIG. 2. Fluorescence for different values of the probe field. Selected parameters are $A_l = 2\gamma$, (a) $\theta = \pi/6$; (b) $\theta = \pi/4$; and (c) $\theta = \pi/3$.

with the experiment [20]. The results of this figure clearly show that the experimentally observed dip at $\Delta = 0$ is due to the saturation produced by both pump and probe fields. Next, results are presented for fluorescence when the probe saturates the atomic transition and the strength of the pump field increases. Fluorescence contributions from populations and coherences are shown separately in Figs. 3(a) and 3(b). Figure 3(c) shows the total fluorescence which is due to both population and interference or coherence contributions. For the direction of observation in this setup, the interference terms are destructive. It is shown that the observed dip at $\Delta = 0$ is the result of the saturation of the transitions by both the pump and probe fields. Furthermore, both populations and coherences contribute to this dip.

In the presence of a magnetic field, the excited levels $|\pm\rangle$ split by $\Delta_B = \pm g\mu B$, where g is the Lande g factor,

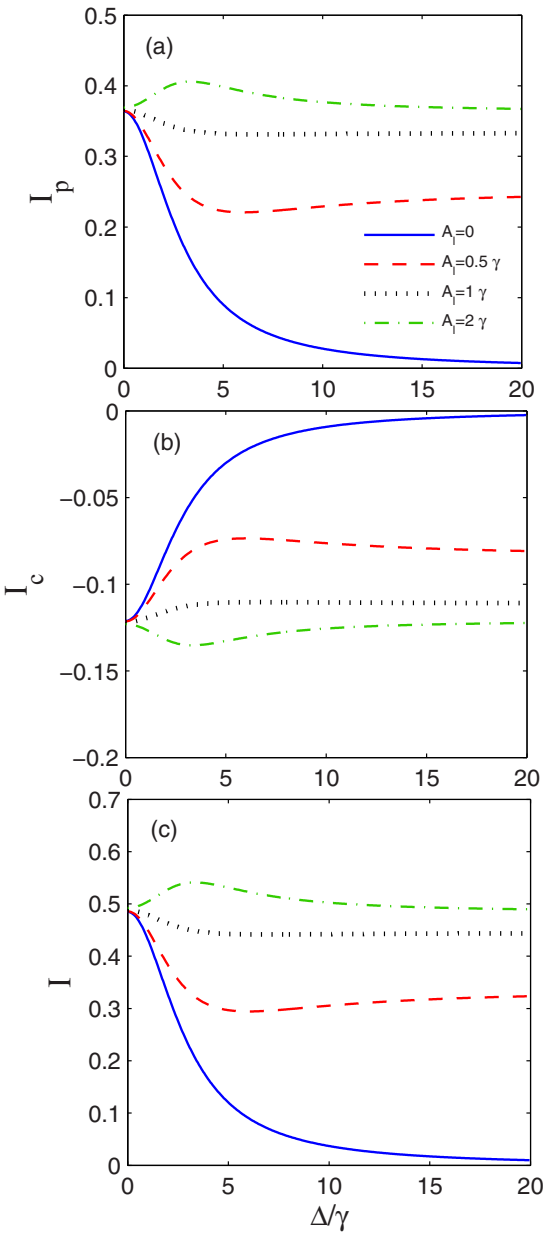

FIG. 3. (a) Population and (b) coherence terms and (c) total magnitude of the fluorescence for different values of the pump field. Parameters used are $\gamma_{+g} = \gamma_{-g} = \gamma_{0g} = \gamma$, $A_p = 2\gamma$, $\delta_{\pm} = \delta_0 = 0$, and $\theta = \pi/4$.

μ is the Bohr magneton, and B is the magnetic field. Now the CPT resonances and CPO resonances separate. The CPO resonances still occur at $\Delta = 0$, but the CPT-like resonances would occur at a position determined by the magnetic field. In Fig. 4, we show the behavior of I as a function of Δ for $\Delta_B = 4\gamma$ and for different values of the Rabi frequencies. The numerical results in Fig. 4 show the general trend seen in the experimental data. In Fig. 5 we present additional results for larger values of the magnetic field. We see a resonant structure at $\Delta \sim \Delta_B$ for low Rabi frequencies. As the pump and probe saturate the atomic transition, a well defined interference minimum is seen at $\Delta \sim \Delta_B$. This is in agreement with the experimental observation. We also see an additional minimum

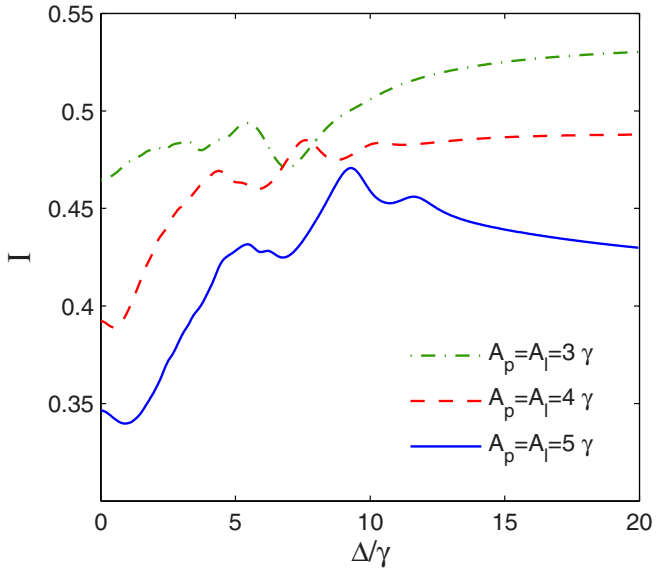

FIG. 4. The fluorescence in the presence of the magnetic field. Parameters used are $\theta = \pi/4$ and $\Delta_B = 4\gamma$. The pump and probe are of equal intensities.

at $\Delta \sim \Delta_B/2$. This additional minimum can be interpreted as a subharmonic resonance. We note that subharmonic resonances were extensively studied in the context of stimulated Raman scattering [22,23]. The subharmonic resonances arise from strong saturation by both pump and probe fields. However, the numerical results do not quite yield the CPT resonance at $\Delta = 2\Delta_B$, as observed in the experiment. It should be borne in mind that the magnetic field can couple the $^3P_1$ level to the $^1P_0$ and $^3P_2$ levels [24,25], and this coupling is most likely the reason why our numerical results do not show the interference minimum at $\Delta = 2\Delta_B$. It may be noted that the magnetic field coupling to such states would be like a phase perturbation and can give rise to interferences similar to collision induced effects [26].

IV. ANALYTICAL RESULTS FOR FLUORESCENCE IN THE ABSENCE OF THE MAGNETIC FIELD

Remarkably enough, the set of Eqs. (5) can be solved analytically in the absence of the magnetic field. Let us make a transformation to a new basis defined by

$$|\psi_1\rangle = \left(\frac{|+\rangle + |-\rangle}{\sqrt{2}}\right)\cos\theta - |0\rangle\sin\theta,$$
$$|\psi_2\rangle = \left(\frac{|+\rangle + |-\rangle}{\sqrt{2}}\right)\sin\theta + |0\rangle\cos\theta,$$
$$|\psi_3\rangle = \frac{|+\rangle - |-\rangle}{\sqrt{2}}. \tag{11}$$

The choice of this basis is determined by the polarization of the pump and probe fields. The states $|\psi_i\rangle (i = 1,2,3)$ form an orthogonal set. The $|\psi_3\rangle$ does not couple to either probe or pump fields. The level $|\psi_2\rangle$ ($|\psi_1\rangle$) couples only to the level $|g\rangle$ by the probe (pump) field. Also, it can be shown that all the decay rates $\gamma_{\psi_1 g}, \gamma_{\psi_2 g}$, and $\gamma_{\psi_3 g}$ are equal to γ. In the new basis the pump and probe fields and spontaneous

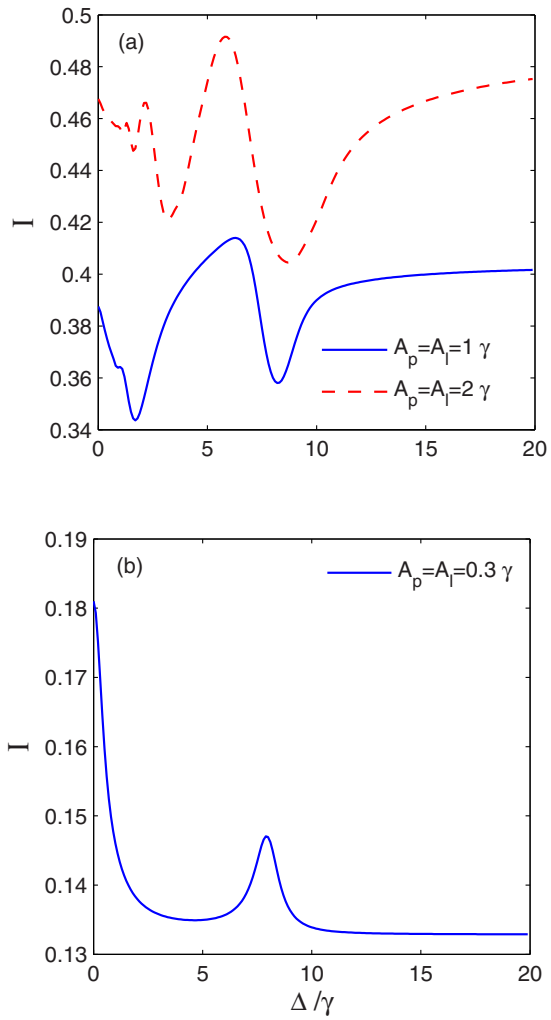

FIG. 5. The fluorescence in the presence of the magnetic field. Parameters used are $\theta = \pi/4$ and $\Delta_B = 8\gamma$. The pump and probe strengths are as shown in the Figures.

emission transitions are shown in Fig. 6. We now rewrite Eqs. (5) in terms of the density matrix elements in the new basis

$$\rho_{\alpha\beta} = \langle\psi_\alpha|\rho|\psi_\beta\rangle. \tag{12}$$

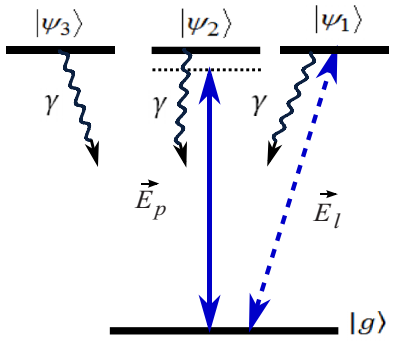

FIG. 6. Schematic diagram of the quantum system in the new basis.

Since the level $|\psi_3\rangle$ is decoupled, it can be dropped from further consideration. The relevant density matrix equations are

$$\begin{aligned}
\dot\rho_{\psi_1\psi_1} &= i\rho_{g\psi_1}A_l - i\rho_{\psi_1 g}A_l - \gamma_{\psi_1 g}\rho_{\psi_1\psi_1},\\
\dot\rho_{\psi_2\psi_2} &= i\rho_{g\psi_2}A_p - i\rho_{\psi_2 g}A_p - \gamma_{\psi_2 g}\rho_{\psi_2\psi_2},\\
\dot\rho_{\psi_1\psi_2} &= -i\Delta\rho_{\psi_1\psi_2} - i\rho_{\psi_1 g}A_p + i\rho_{g\psi_2}A_l - \Gamma_{\psi_1\psi_2}\rho_{\psi_1\psi_2},\\
\dot\rho_{g\psi_1} &= i(\rho_{\psi_1\psi_1} - \rho_{gg})A_l + i\rho_{\psi_2\psi_1}A_p - \Gamma_{g\psi_1}\rho_{g\psi_2},\\
\dot\rho_{g\psi_2} &= -i\Delta\rho_{g\psi_2} + i(\rho_{\psi_2\psi_2} - \rho_{gg})A_p + i\rho_{\psi_1\psi_2}A_l\\
&\quad - \Gamma_{g\psi_2}\rho_{g\psi_2}.
\end{aligned} \tag{13}$$

In deriving Eq. (13), we use a different rotating frame so that no explicit time dependence appears. The state $|\psi_1\rangle$ is rotated with the pump frequency, and the state $|\psi_2\rangle$ is rotated with the probe frequency. The fluorescence in the new basis is given by

$$I = \frac{I_0}{2}[\rho_{\psi_1\psi_1}(1-\cos 2\theta) + \rho_{\psi_2\psi_2}(1+\cos 2\theta)]. \tag{14}$$

The Eqs. (13) are for the V system, and one can solve for arbitrary strengths of the pump and probe fields. The full solutions for $\rho_{\psi_1\psi_1}$ and $\rho_{\psi_2\psi_2}$ are

$$\begin{aligned}
\rho_{\psi_1\psi_1} &= \frac{4A_l^2(N_1+N_2)}{M},\\
\rho_{\psi_2\psi_2} &= \frac{4A_p^2(N_3+N_4)}{M},
\end{aligned} \tag{15}$$

where

$$\begin{aligned}
N_1 &= 4A_p^4 + 4A_l^4 + \gamma^4 + 5\gamma^2\Delta^2 + 4\Delta^4,\\
N_2 &= 4A_l^2(\gamma^2 - 2\Delta^2) + 4A_p^2\left(2A_l^2 + \gamma^2 + 4\Delta^2\right),\\
N_3 &= 4A_p^4 + 4A_l^4 + 4A_p^2\left(2A_l^2 + \gamma^2\right),\\
N_4 &= \gamma^2(\gamma^2 + \Delta^2) + 4A_l^2(\gamma^2 + \Delta^2),\\
M &= 32A_p^6 + 4A_p^4\left(24A_l^2 + 9\gamma^2 + 4\Delta^2\right) + \left(8A_l^2 + \gamma^2\right)\\
&\quad \times\left[4A_l^4 + \gamma^4 + 5\gamma^2\Delta^2 + 4\Delta^4 + 4A_l^2(\gamma^2 - 2\Delta^2)\right]\\
&\quad + 12A_p^2\left[8A_l^4 + \gamma^4 + 2\gamma^2\Delta^2 + 6A_l^2(\gamma^2 + 2\Delta^2)\right].
\end{aligned} \tag{16}$$

Using the analytical results of Eqs. (14) and (15), we have reproduced the numerical results of Figs. 2 and 3. Now, the analytical result can be used to find the strength of the pump and probe for which the interference minimum would appear. For $\theta = \pi/4$, and Δ in the neighborhood of zero, I becomes

$$\begin{aligned}
I = &\frac{4\left(A_p^2 + A_l^2\right)}{8A_p^2 + 8A_l^2 + \gamma^2}\\
&- \frac{16A_p^2\left(2A_p^2 - 6A_l^2 + \gamma^2\right)\Delta^2}{\left(2A_p^2 + 2A_l^2 + \gamma^2\right)\left(8A_p^2 + 8A_l^2 + \gamma^2\right)^2}.
\end{aligned} \tag{17}$$

Clearly for no pump $A_l = 0$, I has a peak at $\Delta = 0$, as can be seen from inspection or from $\frac{\partial^2 I}{\partial\Delta^2} < 0$. The peak crosses over to a dip at a pump power given by

$$A_l^2 > \frac{2A_p^2 + \gamma^2}{6}. \tag{18}$$

Our numerical results in Figs. 2 and 3 are in conformity with the analytical result, Eq. (18).

V. CONCLUSIONS

In this paper, theoretical models of the experiments on coherent population oscillations and coherent population trapping on the intercombination line of ^{174}Yb have been presented. The transition involves a change of the spin and thus can not be interpreted in terms of an effective Λ system which was suggested in [20] using the theoretical framework of [18]. The reported experiments are done in the regime where both pump and probe fields can saturate the transition. We have shown by both numerical and analytical calculations the appearance of the interference minimum as both pump and probe start saturating the transition. We present an analytical result for the threshold probe power required for the interference minimum to appear. It is desirable to have experimental results by scanning both pump and probe powers to show how the interference minimum appears as the threshold, defined by Eq. (18), is crossed. Also, our numerical results show the strong dependence of the interference effects on the angle θ between the probe polarization and the direction of the atomic beam. We also present a detailed study of the appearance of the interference minimum when magnetic fields are applied. Our study also shows the possibility of the appearance of subharmonic resonances in suitable ranges for the pump and probe powers. This finding warrants newer experimental data. The magnetic fields not only create Zeeman splittings, but in addition make the system open because of the couplings to other levels. These couplings give rise to additional resonances in ways similar to dephasing-induced resonances. Newer experiments in this direction are desirable.

[1] E. Arimondo, in *Progress in Optics*, edited by E. Wolf (North Holland, Amsterdam, 1996), Vol. 35, pp. 258–354; G. Alzetta, A. Gozzini, L. Moi, and G. Orriols, Nuovo Cimento B **36**, 5 (1976); E. Arimondo and G. Orriols, Lett. Nuovo Cimento **17**, 333 (1976); H. R. Gray, R. M. Whitley, and C. R. Stroud, Jr., Opt. Lett. **3**, 218 (1978).

[2] L. W. Hillman, R. W. Boyd, J. Krasinski, and C. R. Stroud, Jr., Opt. Commun. **45**, 416 (1983).

[3] K. J. Boller, A. Imamoglu, and S. E. Harris, Phys. Rev. Lett. **66**, 2593 (1991); S. E. Harris, Phys. Today **50**(7), 36 (1997).

[4] O. A. Kocharovskaya and Ya. I. Khanin, Pisma Zh. Eksp. Teor. Fiz. **48**, 581 (1988) [JETP Lett. **48**, 630 (1988)]; S. E. Harris, Phys. Rev. Lett. **62**, 1033 (1989); M. O. Scully, S.-Y. Zhu, and A. Gavrielides, *ibid.* **62**, 2813 (1989); E. S. Fry, X. Li, D. Nikonov, G. G. Padmabandu, M. O. Scully, A. V. Smith, F. K. Tittel, C. Wang, S. R. Wilkinson, and S.-Y. Zhu, *ibid.* **70**, 3235 (1993).

[5] M. O. Scully, Phys. Rev. Lett. **67**, 1855 (1991).

[6] L. V. Hau, S. E. Harris, Z. Dutton, and C. H. Behroozi, Nature (London) **397**, 594 (1999).

[7] S. E. Schwarz and T. Y. Tan, Appl. Phys. Lett. **10**, 4 (1967).

[8] G. S. Agarwal and T. N. Dey, Laser Photon. Rev. **3**, 287 (2009); R. W. Boyd and D. J. Gauthier, in *Progress in Optics*, edited by E. Wolf (North Holland, Amsterdam, 2002), Vol. 43, pp. 497–530.

[9] M. Fleischhauer and M. D. Lukin, Phys. Rev. Lett. **84**, 5094 (2000).

[10] M. A. Maynard, F. Bretenaker, and F. Goldfarb, Phys. Rev. A **90**, 061801 (2014).

[11] K. T. Kapale and G. S. Agarwal, Opt. Lett. **35**, 2792 (2010).

[12] M. O. Scully and M. Fleischhauer, Phys. Rev. Lett. **69**, 1360 (1992).

[13] M. Xiao, Y. Q. Li, S. Z. Jin, and J. Gea-Banacloche, Phys. Rev. Lett. **74**, 666 (1995); F. S. Cataliotti, C. Fort, T. W. Hansch, M. Inguscio, and M. Prevedelli, Phys. Rev. A **56**, 2221 (1997).

[14] M. S. Bigelow, N. N. Lepeshkin, and R. W. Boyd, Phys. Rev. Lett. **90**, 113903 (2003).

[15] G. S. Agarwal and K. T. Kapale, J. Phys. B: At. Mol. Opt. Phys. **39**, 3437 (2006).

[16] J. A. Miles, D. Das, Z. J. Simmons, and D. D. Yavuz, Phys. Rev. A **92**, 033838 (2015).

[17] T. Laupretre, S. Kumar, P. Berger, R. Faoro, R. Ghosh, F. Bretenaker, and F. Goldfarb, Phys. Rev. A **85**, 051805 (2012).

[18] J. Mompart, R. Corbalan, and L. Roso, Phys. Rev. Lett. **88**, 023603 (2002).

[19] In case of Ca the antisymmetric states, that constitute the Λ system, are $|4s,4p_-\rangle$, $|4s,4p_+\rangle$, and $|4p_+,4p_-\rangle$. This leads to the formation of a superposition state of $|4s,4p_-\rangle$ and $|4s,4p_+\rangle$.

[20] A. K. Singh and V. Natarajan, New J. Phys. **17**, 033044 (2015).

[21] G. S. Agarwal, *Quantum Optics* (Cambridge University Press, New York, 2013), Sec. 13.3.1.

[22] G. S. Agarwal, Opt. Lett. **13**, 482 (1988).

[23] R. Trebino and L. A. Rahn, Opt. Lett. **12**, 912 (1987).

[24] L. J. Curtis and D. G. Ellis, J. Phys. B: At. Mol. Opt. Phys. **29**, 645 (1996).

[25] A. V. Taichenachev, V. I. Yudin, C. W. Oates, C. W. Hoyt, Z. W. Barber, and L. Hollberg, Phys. Rev. Lett. **96**, 083001 (2006).

[26] N. Bloembergen, H. Lotem, and R. T. Lynch, Jr., Indian J. Pure Appl. Phys. **16**(3), 151 (1978).